




Structural organization, GABAergic and tyrosine hydroxylase expression in the striatum and globus pallidus of the South American plains vizcacha, *Lagostomus maximus* (Rodentia, Caviomorpha)

Alejandro Raúl Schmidt^{1,3} · Pablo Ignacio Felipe Inerra^{1,3} · Santiago Andrés Cortasa^{1,3} · Santiago Elías Charif^{1,3} · Sofía Proietto^{1,3} · María Clara Corso^{1,3} · Federico Villarreal¹ · Julia Halperin^{1,3} · César Fabián Loidl² · Alfredo Daniel Vitullo^{1,3} · Verónica Berta Dorfman^{1,3} 

Received: 24 May 2019 / Accepted: 6 September 2019 / Published online: 12 September 2019
© Springer Nature B.V. 2019

Abstract

The striatum is an essential component of the basal ganglia that regulates sensory processing, motor, cognition, and behavior. Depending on the species, the striatum shows a unique structure called caudate–putamen as in mice, or its separation into two regions called caudate and lenticular nuclei, the latter formed by putamen and globus pallidus areas, as in primates. These structures have two compartments, striosome and matrix. We investigated the structural organization, GABAergic and tyrosine hydroxylase (TH) expression in the striatum and globus pallidus of the South American plains vizcacha, *Lagostomus maximus*. Its striatum showed regionalization arising from the presence of an internal capsule, and a similar organization to a striosome–matrix compartmentalization. GABAergic neurons in the matrix of caudate exhibited parvalbumin, calretinin, calbindin, GAD65, and NADPH-d-immunoreactivity. These were also expressed in cells of the putamen with the exception of calretinin showing neurofibers localization. Globus pallidus showed parvalbumin- and GAD65-immunoreactive cells, and calretinin- and calbindin-immunoreactive neuropil, plus GABA-A-immunoreactive neurofibers. NADPH-d-, GAD65- and GABA-A-immunoreactive neurons were larger than parvalbumin-, calretinin-, and calbindin-immunoreactive cells, whereas calbindin-immunoreactive cells were the most abundant. In addition, TH-immunoreactive neuropil was observed in the matrix of the striatum. A significant larger TH-immunoreactive area and neuron number was found in females compared to males. The presence of an internal capsule suggests an adaptive advantage concerning motor and cognitive abilities favoring reaction time in response to predators. In an anatomy-evolutionary perspective, the striatum of vizcacha seems to be closer to that of humans than to that of laboratory traditional models such as mouse.

Keywords Striatum · GABA · Tyrosine hydroxylase · Sexual dimorphism · Vizcacha

Introduction

The basal ganglia are composed of the striatum, globus pallidus, subthalamic nucleus and substantia nigra (Smith et al. 1998; Shipp 2017). Within these structures, the striatum (caudate nucleus and putamen) present two distinguishable types of compartment, striosomes (or patches) that form a labyrinthine and interconnected structure, and matrix that keeps and surrounds the striosomes (Graybiel and Ragsdale 1978; Herkenham and Pert 1981; Gerfen 1984). Both compartments have specific properties with GABAergic, dopaminergic and nitroergic neurons (Graybiel and Ragsdale 1978; Sandell et al. 1986; Graybiel 1983, 1990; Kubota and Kawaguchi 1993; Holt et al. 1997). The striatum is involved in motor and cognitive functions (DeLong

✉ Verónica Berta Dorfman
dorfman.veronica@maimonides.edu

¹ Centro de Estudios Biomédicos, Biotecnológicos, Ambientales y Diagnóstico (CEBBAD), Universidad Maimonides, Hidalgo 775 6to piso, C1405BCK Ciudad Autónoma de Buenos Aires, Argentina

² Laboratorio de Neuropatología Experimental, Instituto de Biología Celular Y Neurociencia (IBCN) “Prof. E. De Robertis”, Facultad de Medicina, Universidad de Buenos Aires, CONICET, Ciudad Autónoma de Buenos Aires, Argentina

³ Consejo Nacional de Investigaciones Científicas Y Técnicas (CONICET), Buenos Aires, Argentina

and Georgopoulos 1981; DeLong et al. 1984; Middleton and Strick 1994). In order to build motor patterns based on the environment information as well as on past experience, the striatum integrates the incoming information from all regions of the cerebral cortex (Graybiel 2008). This structure receives inputs from the dopaminergic, glutamatergic and serotonergic systems coming different areas of the brain, including the cortex, mesencephalon, and thalamus (Kubota et al. 1986; Lavoie and Parent 1990; Fujiyama et al. 2006; Kawaguchi et al. 1995). On the other hand, its GABAergic efferents show stimulating or inhibitory effects on movement according to their projection through direct or indirect pathways. In those pathways, the internal and external globus pallidus are involved, respectively (Gerfen and Wilson 1996; Smith et al. 1998; Gillies et al. 2002; Micheli and Luquin-Piudo 2012; Kita and Jaeger 2016).

The structural organization of the striatum differs among species. In rodents such as mice and rats, the striatum is a unique structure formed by the caudate and putamen areas called caudate-putamen, without internal defined limits (Paxinos and Franklin 2004). However, in primates, the presence of a tract of white matter crossing the striatum, called internal capsule, separates the caudate-putamen into two regions: caudate and lenticular nuclei, the latter formed by putamen and globus pallidus areas (Carpenter 1994; Snell 2007).

The South American plains vizcacha, *Lagostomus maximus*, is a basal hystricognathe rodent belonging to the family Chinchillidae (Fig. 1), distributed in the Pampas region of Argentina extending up to the South of Paraguay and Bolivia (Jackson et al. 1996). This species is a large herbivore fossorial rodent living in communal burrow systems with nocturnal foraging outings (Llanos and Crespo 1952). Night-time outputs expose them to predation, especially by puma (*Puma concolor*) and, eventually, by smaller felids like the Geoffroy's cat (*Oncifelis geoffroyi*). However, the attack success of predators on vizcacha is low, around 10% (Branch 1995). Vizcachas convert dense grass around burrows to low-growing forbs which together with loud warning vocalization prevent predators to get close enough for a successful ambush (Branch 1993a, 1995). Although these behaviors are supposed to be the main strategy against predation, in situ observation of predator-vizcacha interaction has shown that they have sensorial and motor skills that guarantee their quick escape (Branch 1995). Much of the processing information on those skills involves the striatum, acting together with the cortex and the cerebellum.

Up to the present, there have been no studies on the striatum in the vizcacha or other Chinchillidae, which are at the base of rodent phylogeny (Fig. 1b). The aim of the present work was to analyze the structural organization and GABAergic expression of the striatum and globus pallidus of the vizcacha. We also evaluated the possible existence

of dopaminergic sexual dimorphism. We discuss the results in the light of habits and behaviour of the species, and the possible evolutionary meaning of the striatum's anatomy.

Materials and methods

Animals

Adult plains vizcachas were captured from a resident natural population at the *Estación de Cría de Animales Silvestres* (ECAS), Villa Elisa, Buenos Aires, Argentina using live-traps located at the entrance of their burrows. All experimental protocols concerning animal handling were conducted in accordance with the guidelines published in the National Institutes of Health (NIH) guide for the care and use of laboratory animals (National Research Council USA 2011), and were reviewed and approved by the Institutional Committee on Use and Care of Experimental Animals (CICUAE) from Universidad Maimónides, Argentina (Resolution N°16/14). The capture and transport of animals were approved by the Ministry of Agriculture Authority of the Buenos Aires Province Government. Appropriate procedures were performed to minimize the number of animals used. Adult non-pregnant non-ovulating females ($n = 13$; 2.2–3.5 kg body weight) were captured in March according to the natural reproductive cycle described by Llanos and Crespo (1952), and our own previous field expertise (Jensen et al. 2006; Dorfman et al. 2011, 2013; Halperin et al. 2013; Charif et al. 2016, 2017; Inserra et al. 2017). Adult males with testicular recrudescence ($n = 7$; 4.5–6.5 kg body weight) were captured in June (González et al. 2012a, b, 2018). All animals ranged from 2.5 to 3.5 years old as determined by the dry crystalline lens weight according to Jackson (1986). The data for the single animals were introduced in Table 1.

Tissue collection

Animals were anaesthetized by the intramuscular injection of 13.5 mg/kg body weight ketamine chlorhydrate (Holliday Scott S.A., Buenos Aires, Argentina) and 0.6 mg/kg body weight xylazine chlorhydrate (Richmond Laboratories, Veterinary Division, Buenos Aires, Argentina) and sacrificed by an intracardiac injection of 0.5 ml/kg body weight of Euthanyl™ (Sodic Pentobarbital, SodicDiphenilhidanthoine, Brouwer S.A., Buenos Aires, Argentina); brains were immediately removed and processed (see below).

Histological staining

After removal, brains were serially sectioned in a coronal plate in 5 mm thick blocks, immediately fixed in cold 4% paraformaldehyde (PFA) (Sigma Aldrich Inc., St. Louis,

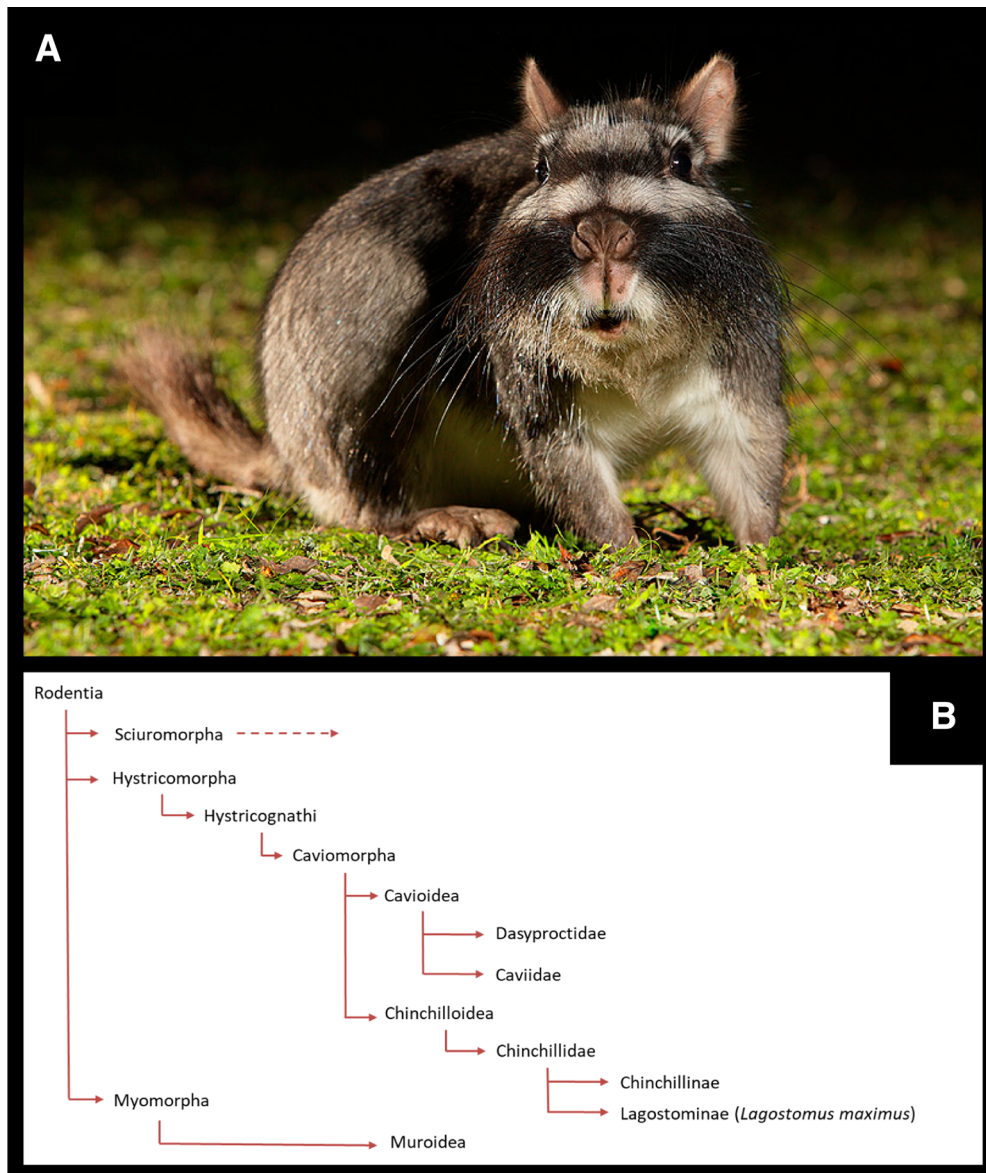


Fig. 1 The South American plains vizcacha, *Lagostomus maximus*, and the phylogenetic tree of the Rodentia. Photograph of a wild vizcacha specimen. Courtesy of Francisco Rebollo Paz (a). Cladogram of the order Rodentia with the suborders Sciuromorpha, Hystrico-

morpha and Myomorpha. In the Hystricomorpha suborder, within the Hystricognathi infraorder, parvorden Caviomorpha, at Chinchilloidea superfamily, Chinchillidae family, Lagostominae subfamily is located, the species *Lagostomus maximus* belongs (b)

Missouri, USA) in 0.1 M phosphate-buffer saline (PBS) (pH 7.4) for 72 h, dehydrated through a graded series of ethanol and embedded in paraffin. For each specimen, the block containing the brain region comprising the striatum was entirely cut in serial coronal sections (5 μm thick) with a microtome (Leica RM2125RT, Wetzlar, Germany) and mounted individually onto coated slides. Sections were dewaxed in xylene and rehydrated through a decreasing series of ethanol (100, 95 and 70%). One every seven slides was separated to visualize neurons by classical Nissl staining using cresyl violet solution (0.1 g/l crystal

violet in 10% glacial acetic acid, pH 7.4), and myelin by Klüver–Barrera staining using 0.1 g/l Luxol fast blue and 0.05 g/l lithium carbonate plus counterstaining with cresyl violet solution (Klüver and Barrera 1953). The location of the striatum was established by comparison with rat (*Rattus norvegicus*), mouse (*Mus musculus*), chinchilla (*Chinchilla lanigera*) and guinea pig (*Cavia porcellus*) histological brain atlases (Tindal 1965; Luparello et al. 1964; Paxinos and Franklin 2004; Paxinos and Watson 2013); according to the anatomical characteristics, three levels of striatum (rostral, mid, and caudal) were established.

Table 1 Single data of experimental animals

| Vizcacha number | Sex | Body mass (kg) | Brain mass (g) | Years | Technique |
|-----------------|--------|----------------|----------------|-------|-----------|
| 102063 | Male | 6.45 | 15.58 | 3.50 | IHQ |
| 107393 | Male | 4.50 | 14.80 | 3.00 | IHQ |
| 107403 | Male | 6.00 | 15.43 | 3.45 | IHQ |
| 107533 | Male | 5.50 | 15.30 | 3.20 | IHQ |
| 109203 | Male | 4.80 | 15.10 | 3.00 | IHQ |
| 109933 | Male | 4.50 | 14.50 | 2.80 | WB |
| 112073 | Female | 2.90 | 13.80 | 2.50 | IHQ |
| 112123 | Female | 3.20 | 12.60 | 3.00 | IHQ |
| 117553 | Female | 3.30 | 13.10 | 3.10 | IHQ |
| 117563 | Female | 2.30 | 12.20 | 2.50 | IHQ |
| 118263 | Female | 2.55 | 13.56 | 2.60 | IHQ |
| 118293 | Female | 2.90 | 13.80 | 3.00 | IHQ |
| 118903 | Female | 2.60 | 13.48 | 2.80 | NADPH-d |
| 119023 | Female | 2.95 | 14.00 | 3.00 | NADPH-d |
| 119263 | Female | 3.50 | 14.06 | 3.50 | NADPH-d |
| 119273 | Female | 3.30 | 13.90 | 3.40 | WB |

IHQ immunohistochemistry, *NADPH-d* NADPH-diaphorase staining, *WB* Western-blot

Immunohistochemistry

All the sections from mid-striatum were dewaxed in xylene and rehydrated through a decreasing series of ethanol (100, 95 and 70%). Antigen retrieval was performed boiling sections in 10 mM sodium citrate buffer (pH 6) for 20 min, followed by 20 min cooling at room temperature. Then, endogenous peroxidase activity was blocked with 2% hydrogen peroxide in methanol for 20 min. After that, sections were incubated with blocking solution of PBS containing 10% normal serum (pH 7.4) for 1 h. Immunoreactivity was detected incubating slides overnight at room temperature with the corresponding primary antibody (Table 2). Specificity was corroborated in adjacent sections by omission of the primary antibodies. Immunoreactivity was revealed with biotinylated goat anti-rabbit IgG or with biotinylated horse anti-goat IgG followed by incubation with avidin–biotin complex (ABC Vectastain Elite kit, Vector Laboratories, Burlingame, California, USA). The reaction was visualized with 3,3'-diaminobenzidine (DAB) and intensified with nickel ammonium sulphate (DAB kit, Vector Laboratories, Burlingame, California, USA) that yields a black product.

Finally, sections were dehydrated through a graded series of ethanol (70%, 95% and 100%), cleared in Neo-Clear (Merck KGaA, Darmstadt, Germany) and cover slipped. Six females and five males were tested.

NADPH-diaphorase histochemistry

After removal, brains were coronally sectioned in blocks of 5–6 mm thick and fixed in cold 4% PFA in 0.1 M PBS (pH 7.4) for 72 h, cryoprotected in 30% sucrose in 0.1 M phosphate buffer, frozen with powdered dry ice and stored at -80°C . Brain regions containing the striatum were entirely cut with a cryostat (Leica CM1850, Wetzlar, Germany) to serial coronal sections (20 μm thick), mounted onto coated slides, air dried and stored at -80°C . In order to identify sections containing mid-striatum, classical Nissl staining was performed in one out of ten adjacent sections. Sections were incubated with a solution containing 0.1% β -NADPH and 0.02% nitroblue tetrazolium diluted in 0.1 M phosphate buffer, pH 7.4, with 0.3% Triton X-100, for 60 min at 37°C . Negative control was performed omitting NADPH in the incubation mixture. Three females were used.

Table 2 Primary antibodies

| Target | Species | Dilution | Source | Reference |
|----------------------|-------------------|----------|--------------------|-----------|
| Calbindin D28K | Rabbit polyclonal | 1:200 | Santa Cruz Biotech | sc-7691 |
| Calretinin (H-5) | Mouse monoclonal | 1:200 | Santa Cruz Biotech | sc-365956 |
| GABA A Ra1-6 (E-8) | Mouse monoclonal | 1:200 | Santa Cruz Biotech | sc-376282 |
| GAD-65 (A-3) | Mouse monoclonal | 1:200 | Santa Cruz Biotech | sc-377145 |
| Parvalbumin a (C-19) | Goat polyclonal | 1:200 | Santa Cruz Biotech | sc-7449 |
| Tyrosine hydroxylase | Rabbit polyclonal | 1:200 | Millipore | AB152 |

Image analysis and quantification approach

Anatomically matching areas among animals were selected for the image analysis. Microscope images of histological, histochemical and immunoreactive staining were captured with an optic microscope (BX40, Olympus Optical Corporation, Tokyo, Japan), fitted with a digital camera (390CU 3.2 Megapixel CCD Camera, Micrometrics, Spain), and the image software Micrometrics SE P4 (Standard Edition Premium 4, Micrometrics, Spain). To avoid variations in the determination of the specific immunoreactivity and in the quantification process, all the images for the same marker were obtained the same day and under the same light and contrast intensity. Immunoreactive cells and NADPH-d reactive cells were quantified with Image-Pro Plus software (Image-Pro Plus 6, Media Cybernetics Inc., Bethesda, Maryland, USA). In order to check the distribution of each marker through the mid-striatum three females were used. In these cases, all the tissue sections containing the mid-striatum (50 sections) were analyzed. Each of the six antibodies employed was used in a systematic manner in consecutive sections followed by the two sections used for Nissl staining and for Klüver–Barrera staining. This sequence was systematically six times repeated in order to cover all the mid-striatum. In this way, six sections distributed throughout the whole mid-striatum were stained for each antibody and cells expressing each marker were counted every eight sections. In the remaining three females and in the five males, measures were assayed in just three slices distributed at the rostral, middle and caudal regions of the mid-striatum. In order to be comparable with the former mentioned analyzed slices, sections were chosen in a systematic manner, spaced at an interval of 120 μm from each other within the striatum. At each section, absolutely all the immunostained cells were measured in an exhaustive fashion. The analyses were conducted in both left and right sides of the brains. For each area (caudate, putamen or globus pallidus) the density of immunoreactive cells (NRC, expressed as the average of the number of immunoreactive cells/10 mm^2), the somatic reactive area (SRA, expressed in μm^2) and the medial diameter of reactive cells (MDRC, expressed in μm) were determined using the staining optical density. Only those cells that had a grey level darker than a defined threshold criteria (defined as the optical density threefold higher than the mean background density) were considered as specific immunoreactive stained cells. The background density was measured in a region devoided of immunoreactivity, immediately adjacent to the analyzed region. The SRA and the MDRC were determined as the surface covered by the pixels that exceed the threshold density criterion. Similar methods were previously employed by our group (Dorfman et al. 2013) and by others (Rey-Funes et al. 2013, 2016). The measurements informed as SRA and MDRC have been corrected

by the tissue shrinkage and swelling factor which did not vary between males and females. Regarding to GAD-65, in spite that mild-stained cells with a very low optical density were observed, only those cells showing an optical density that exceed the defined threshold criteria were considered for the quantification (referred to as strong-stained). On the other hand, in order to detect a possible sexual dimorphism, the percentage of the TH-immunoreactive area ($\text{IRA} = \text{TH-immunoreactive area/caudate plus putamen areas}$) and the number of TH-immunoreactive neurons/10 mm^2 of striatum were determined in male and female vizcachas. TH-immunoreactive area was determined using the optical density. The area that had a grey level darker than the defined threshold criteria was considered for the quantification. Quantifications were done by two independent observers. Adobe Photoshop software (Adobe Photoshop CS5, Adobe Systems Inc., Ottawa, Ontario, Canada) was used for digital manipulation of brightness and contrast when preparing the shown images.

Sodium dodecylsulphate polyacrylamide gel electrophoresis (SDS)-PAGE and Western-blotting

Immediately after brain removal, striatum was homogenized (1:3 w/v) in RIPA buffer (0.1 M PBS with 1% Igepal, 0.5% sodium deoxycolate and 0.1% SDS, pH 7.4), containing 0.1 μM aprotinin, 0.1 μM leupeptin, 0.1 μM pepstatin and 0.1 mM phenyl methyl sulfonyl fluoride (PMSF). All procedures were carried out at 4 °C. Homogenate was centrifuged for 30 min at 14,000 $\times g$ and supernatant collected. Protein concentration was determined by Bradford method (Bradford 1976) using bovine serum albumin (BSA) as a standard. Fifty micrograms of solubilized proteins were mixed with sample buffer (1 M Tris–HCl with 10% w/v SDS, 30% v/v glycerol, 0.1% w/v bromo phenol blue and 0.15% w/v 2-mercaptoethanol, pH 6.8) and heated for 3 min at 100 °C. Proteins were separated on an SDS–polyacrylamide 10% running gel and 4% stacking gel (29:1 acrylamide: bis acrylamide, Bio-Rad Laboratories, Hercules, California, USA), with 0.25 M Tris–glycine, pH 8.3, as the electrolyte buffer, in an electrophoresis cell (Mini-PROTEAN II Electrophoresis Cell, Bio-Rad Laboratories, Hercules, California, USA). For Western-blot analysis, proteins were electrotransferred to a 0.2 mm polyvinylidene difluoride (PVDF) membrane (Immobilon-P, EMD Millipore Corporation, Billerica, Massachusetts, USA) at 400 mA for 75 min. For protein identification, membranes were blocked 1 h at room temperature with 5% powdered skim milk in PBS containing 0.1% Tween 20. Then, they were incubated overnight at 4°C with the appropriate primary antibody (1:200 dilution, Table 2). For immunoreactivity development, membranes were incubated with goat anti-rabbit IgG–HRP (1:3000 dilution, 170–6515, Bio-Rad Laboratories, California, USA),

with anti-mouse IgG-HRP (1:3000 dilution, sc-516102, m-IgG κ BP-HRP, Santa Cruz Biotechnology, Santa Cruz, California, USA), or with horse anti-goat IgG-HRP (PI-9500, Vector Laboratories, California, USA) as appropriate. For chemiluminescence development, ECL Plus kit (GE Healthcare Ltd., Amersham Place, Buckinghamshire, United Kingdom) was employed. Membranes were scanned with a ImageQuant 350 Capture Imaging System (GE Healthcare Bio-Sciences AB, Uppsala, Sweden). The estimation of the band size was performed using a pre-stained protein ladder (PageRuler, Fermentas UAB, Vilnius, Lithuania) as molecular weight marker. In this technique, two pools of proteins were used: one pool of proteins extracted from two striatum of rats (one male and one female) and another pool of proteins extracted from two striatum of vizcachas (one male and one female).

Statistical analysis

Values are expressed as the average among animals \pm mean standard deviation. Results of dimorphism were evaluated using *t*-test for comparisons between two groups. Differences were considered significant when $p < 0.05$. Statistical analysis was performed using Prism 4.0 software (GraphPad Software Inc., San Diego, California, USA).

Results

Anatomical and histochemical description of the striatum of the vizcacha

The striatum was dorsally delimited by the extension of the white matter that separates the striatum from the brain cortex, laterally by the extension of the white matter forming the external capsule and internally by the lateral ventricle and a band of white matter forming the internal capsule, and ventrally by the amygdaloid area (Fig. 2). The morphology of the striatum was studied in a rostro-caudal orientation, and the rostral-, mid-, and caudal-striatum levels were analyzed. Both rostral- and caudal-striatum showed homogenous morphology forming a unique caudate-putamen structure (Fig. 2a–c, g–i). However, at the mid-striatum level (spanning about 300 μ m), an internal capsule dividing the caudate-putamen structure in caudate and putamen was observed (Fig. 2d–f). At the three levels, caudate and putamen showed a similar organization to a striosome-matrix compartmentalization. A schematic representation of coronal sections at rostral-, mid- and caudal-striatum, and the regionalization of the mid-striatum into caudate and putamen areas is shown in Fig. 2c, f, i.

GABAergic system expression in the mid-striatum and globus pallidus of the vizcacha

Considering the regionalization of the mid-striatum of the vizcacha, the distribution and the relative abundance of cells expressing different components of the GABAergic system were analyzed. GABAergic expression was determined in the three areas caudate, putamen and globus pallidus of non-pregnant females. Homogenous distribution of each marker was determined along the rostro-caudal extension of complete mid-striatum. Three females were used (Fig. 3). Considering this homogenous distribution, GABAergic system inspection for the remaining animals was developed in three representative tissue sections corresponding to rostral, middle, and caudal regions of the mid-striatum respectively. Specific expression was determined at caudate, putamen and globus pallidus for each studied marker.

Parvalbumin

Parvalbumin-immunoreactivity, which indicates the presence of GABAergic aspiny interneurons, was observed in cells localized in the matrix of the caudate and putamen as well in the globus pallidus (Fig. 4a–c). The putamen showed the largest number of immunoreactive cells whereas the caudate displayed the lowest number (Table 3). In addition, cells from globus pallidus were smaller than the cells from other two areas (Table 3).

NADPH-d

NADPH-d stained cells, which evidences the presence of GABAergic aspiny interneurons, were distributed in the matrix of both caudate and putamen (Fig. 4d–e). Big and scarce NADPH-d stained bipolar or multipolar neurons, with primary and secondary ramifications, were detected. Caudate and putamen exhibited a similar number of NADPH-d stained neurons (8 ± 2 and 9 ± 3 , respectively), whereas NADPH-d cells at both areas showed similar size (caudate: $104.09 \pm 25.02 \mu\text{m}^2$ somatic reactive area and $11.45 \pm 1.37 \mu\text{m}$ medial diameter; putamen: $144.06 \pm 52.04 \mu\text{m}^2$ somatic reactive area and $13.75 \pm 3.01 \mu\text{m}$ medial diameter). The globus pallidus was devoid of NADPH-d stained cells. Only randomly distributed microvessels were detected in this area (Fig. 4f).

Calretinin

Calretinin, a marker of GABAergic aspiny interneurons, was differentially detected in the matrix or in the patches depending of the nucleus. In the caudate, clusters of round-shaped calretinin-immunostained neurons with labelling in the proximal segment of some dendrites, were

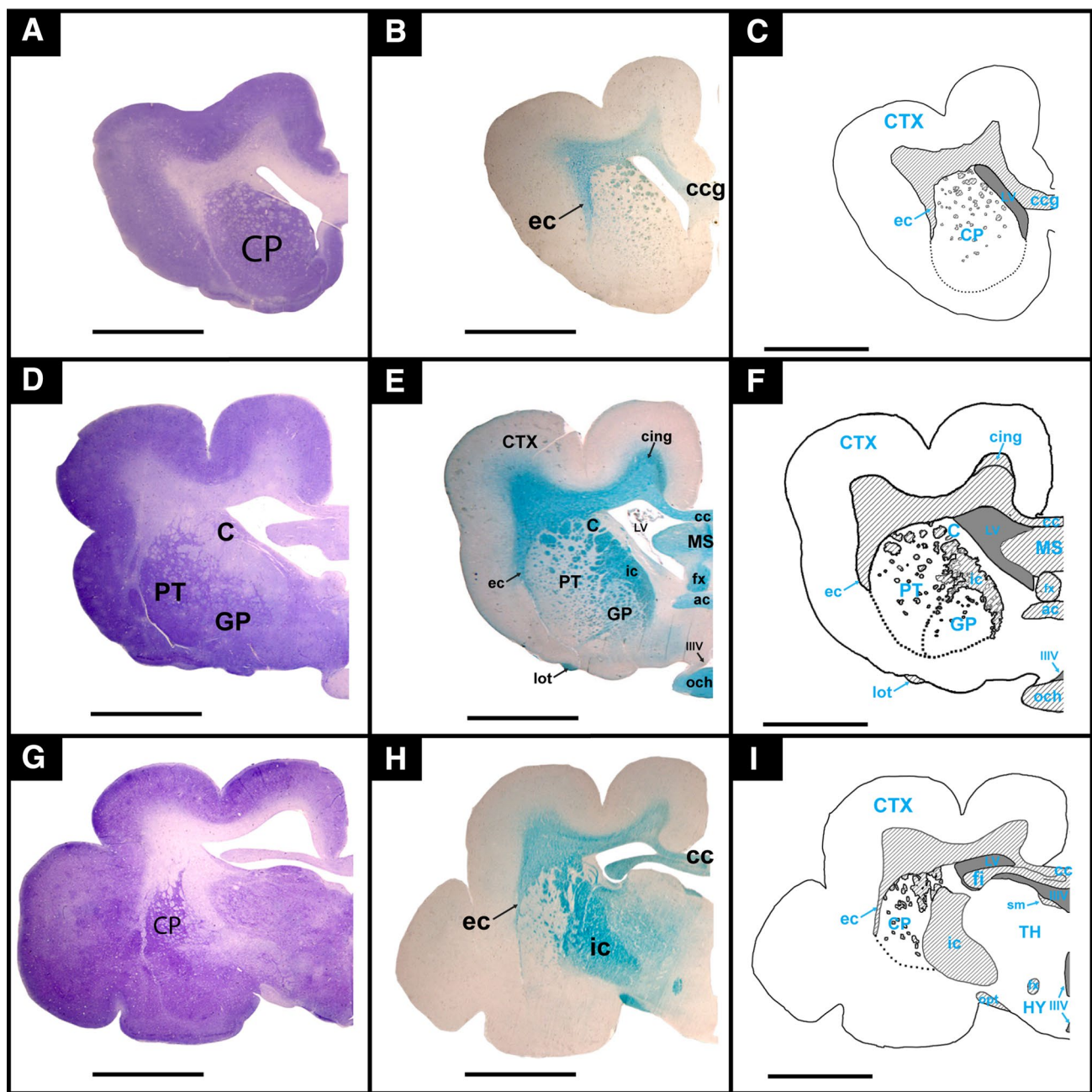


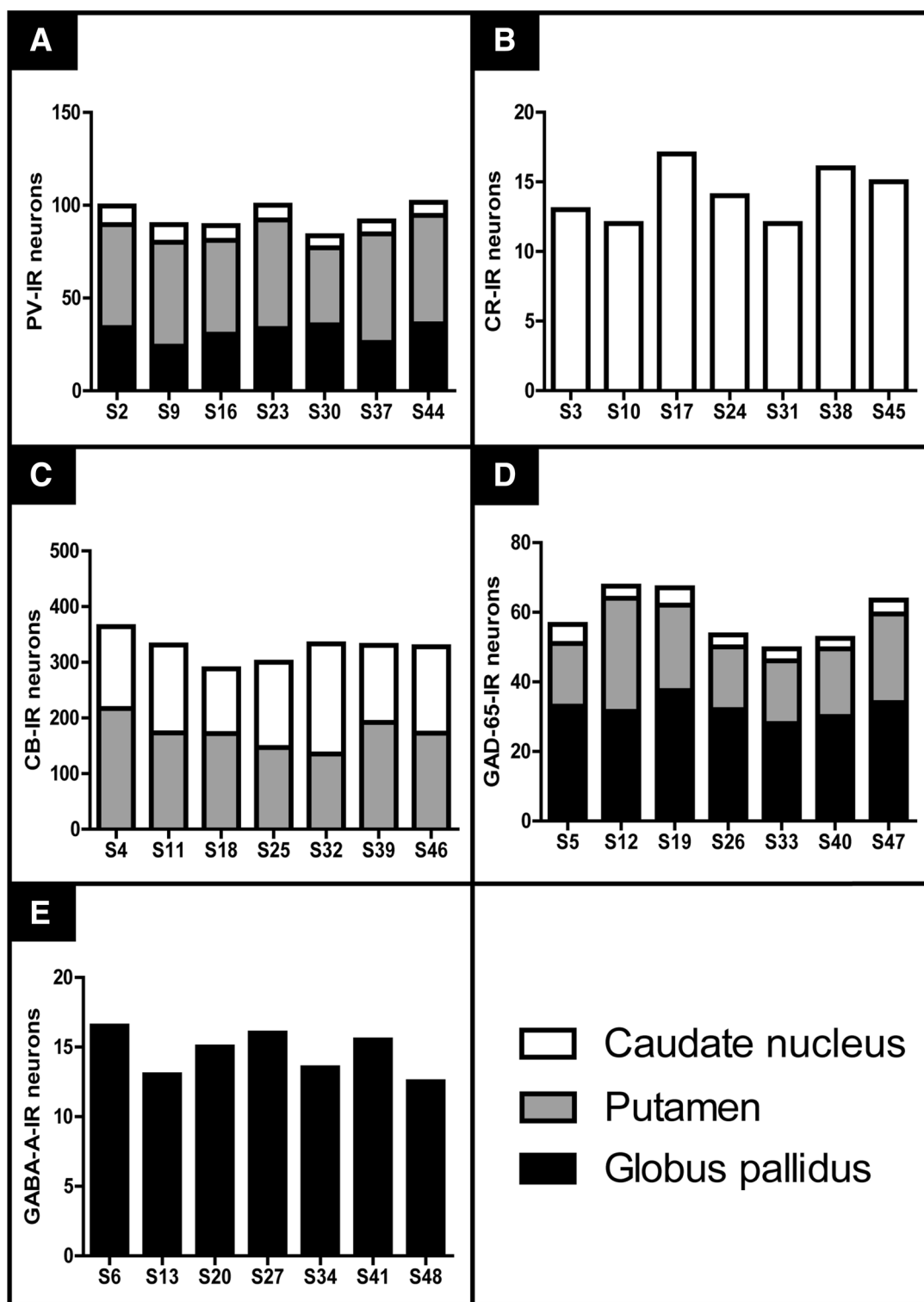
Fig. 2 Structural organization of the striatum of the vizcacha, *Lagostomus maximus*. Representative images of coronal hemi-sections showing the localization of the rostral-striatum (**a–c**), mid-striatum (**d–f**) and caudal-striatum (**g–i**). **a, d** and **g** Nissl staining; **b, e** and **h** Kliver–Barrera technique; **c, f, i** Schematic representation showing the striatum regionalization in caudate nucleus and putamen. White matter (lined), gray matter (white) and ventricles (grey) are shown.

ac: anterior commissure; C: caudate nucleus, cc: corpus callosum, ccg: corpus callosum genu, cing: cingulate, CP: caudate-putamen, CTX: cortex, ec: external capsule, fx: fornix column, GP: globus pallidus, ic: internal capsule, IIIV: 3rd ventricle, lot: lateral optical tract, LV: lateral ventricle, MS: medial septal nucleus, och: optic chiasm, PT: putamen. Scale bars: 5 mm

distributed in the matrix (Fig. 4g, and Table 3), whereas the putamen showed calretinin-immunoreactive neurofibers with patch localization (Fig. 4h). The globus pallidus revealed calretinin-immunoreactivity in neuropil (Fig. 4i).

Calbindin

Calbindin, a marker of GABAergic spiny neurons, presented immunoreactivity at neuropil and cells of matrix.



Abundant round-shaped neurons with the proximal segment of their dendrites positively labeled for calbindin were localized in the matrix of both caudate and putamen with similar abundance and size (Fig. 5a–c and Table 3).

Glutamic acid decarboxilase 65 (GAD65)

The expression of GAD65, the enzyme involved in γ -aminobutyric acid (GABA) synthesis, showed two subpopulations of GAD-65 neurons, with mild- or strong-staining, in striatum and globus pallidus (Fig. 5d–f). Only

Fig. 3 Distribution of GABAergic cells throughout the entire section of mid-striatum and globus pallidus of female vizcacha, *Lagostomus maximus*. Parvalbumin (a), calretinin (b), calbindin (c), GAD-65 (d), and GABA-A (e)—immunoreactivity was evaluated in the entire section of mid-striatum and globus pallidus of female vizcacha. The complete mid-striatum was studied in its rostro-caudal orientation and all the sections (a total of 50) were stained for immunohistochemistry. Each antibody was used in consecutive sections, and this sequence was seven times repeated in order to cover all the mid-striatum. In this way, cells expressing each marker were systematically counted every seven sections. For each marker, bars represent the number of immunoreactive cells corresponding to the whole striatum, whereas the number of immunoreactive cells in caudate nucleus, putamen and globus pallidus was white, grey and black represented. *CB* calbindin, *CR* calretinin, *GABA-A* γ -aminobutyric acid ionotropic receptor, *GAD-65* glutamic acid decarboxylase 65, *IR* immunoreactive, *S* section, *PV* parvalbumin

the big GAD-65 immunoreactive cells with six times higher optical density than the background were quantified (referred to as strong-stained). The caudate nucleus and the putamen depicted abundant mild stained round multipolar neurons together with scarce strong stained cells, whereas the globus pallidus showed scarce mild stained cells together with abundant strong stained fusiform-bipolar neurons (Fig. 5d–f and Table 3).

GABA ionotropic receptor A (GABA-A)

Immunoreexpression of GABA-A was detected in the neuropil of the caudate nucleus and putamen, but GABA-A immunolabeled cells were not detected in those areas (Fig. 5g–i). The globus pallidus displayed large scarce bipolar GABA-A immunoreactive neurons immersed among immunopositive neurofilaments (Fig. 5i and Table 3).

Specific immunoreactivity was not detected when adjacent slides were incubated in the same conditions but omitting the primary antibodies (Fig. 6g–i). In addition, single bands corresponding to the expected molecular weights of parvalbumin, calretinin, calbindin, GAD 65, and GABA-A were detected by Western-blot in a protein extract from the striatum of a female vizcacha and a female rat (Fig. 6a–e). This reproducible pattern between vizcacha and rat, and the single band obtained for each marker, reinforced the specificity of the employed antibodies.

Sexual dimorphism for tyrosine hydroxylase expression in the mid-striatum of the vizcacha

Tyrosine hydroxylase (TH) expression, a marker of dopamine synthesis intermediary, was studied throughout striatum. The darkest TH optical density was detected at the matrix of caudate, whereas the matrix of putamen showed a lower intensity of TH-immunoreactivity (Fig. 7a). A fibrillar TH-immunoreactive pattern was observed in the matrix

of the striatum and in the globus pallidus (Fig. 7b–d). In the caudate nucleus, TH-immunoreactive nerve endings were detected around TH immunonegative neurons (Inset Fig. 7b), whereas a few and small TH-immunoreactive cells were detected in putamen (Fig. 7c). In the globus pallidus, sparse TH-immunoreactive axonic varicosities were observed (Fig. 7d). TH-immunoreactivity was not detected when adjacent slides were incubated in the same conditions but omitting the primary antibody (Fig. 6g). Since TH-immunoreactivity was previously shown to be sexually dimorphic in other rodents (Leranth et al. 2000; Daubner et al. 2011), here we compared TH expression between male and female vizcachas. Females showed a significant larger mid-striatum TH-immunoreactive area than males (10% of increment) (Fig. 7e) and a significantly higher abundance of TH-immunoreactive cells that were only identified in the putamen (Fig. 7f). Significant differences between sexes were not found in the size of TH-immunoreactive cells (females: $11.26 \pm 3.87 \mu\text{m}^2$ somatic reactive area and $3.79 \pm 0.56 \mu\text{m}$ medial diameter; males: $12.13 \pm 2.18 \mu\text{m}^2$ somatic reactive area and $4.01 \pm 0.42 \mu\text{m}$ medial diameter).

In a Western-blot assay, single bands corresponding to the expected molecular weight were detected for TH (60 kDa) in the striatum of vizcacha and rat (Fig. 6f). This reproducible pattern between vizcacha and rat, and the single band obtained, reinforced the specificity of the anti-TH employed antibody.

Discussion

The present work describes for the first time the striatum of the South American plains vizcacha showing its regionalization, compartmentalization and GABAergic expression in the striatum. The striatum structural organization greatly differs from that described for miomorph rodents and it relates the basal histocognate vizcacha to other taxa sharing a common ancestor. Besides, TH immunoreactivity revealed the existence of dopaminergic sexual dimorphism.

GABAergic characterization of mid-striatum

In order to describe the GABAergic expression in the mid-striatum of the vizcacha, several markers previously used for striatal characterization in other species like mouse, rat, cat (*Felis silvestris*), gerbil (*Meriones unguiculatus*), tree shrew (*Anathana ellioti*), monkey (*Saimiri sciureus*) and human were studied (Sandell et al. 1986; De Las Heras et al. 1994; Holt et al. 1997; Wu and Parent 2000; Rice et al. 2011; Bae et al. 2015). Spiny and aspiny GABAergic neurons have been described in the mid-striatum of the vizcacha: spiny neurons expressing calbindin and sending projections from both caudate and putamen regions towards the globus

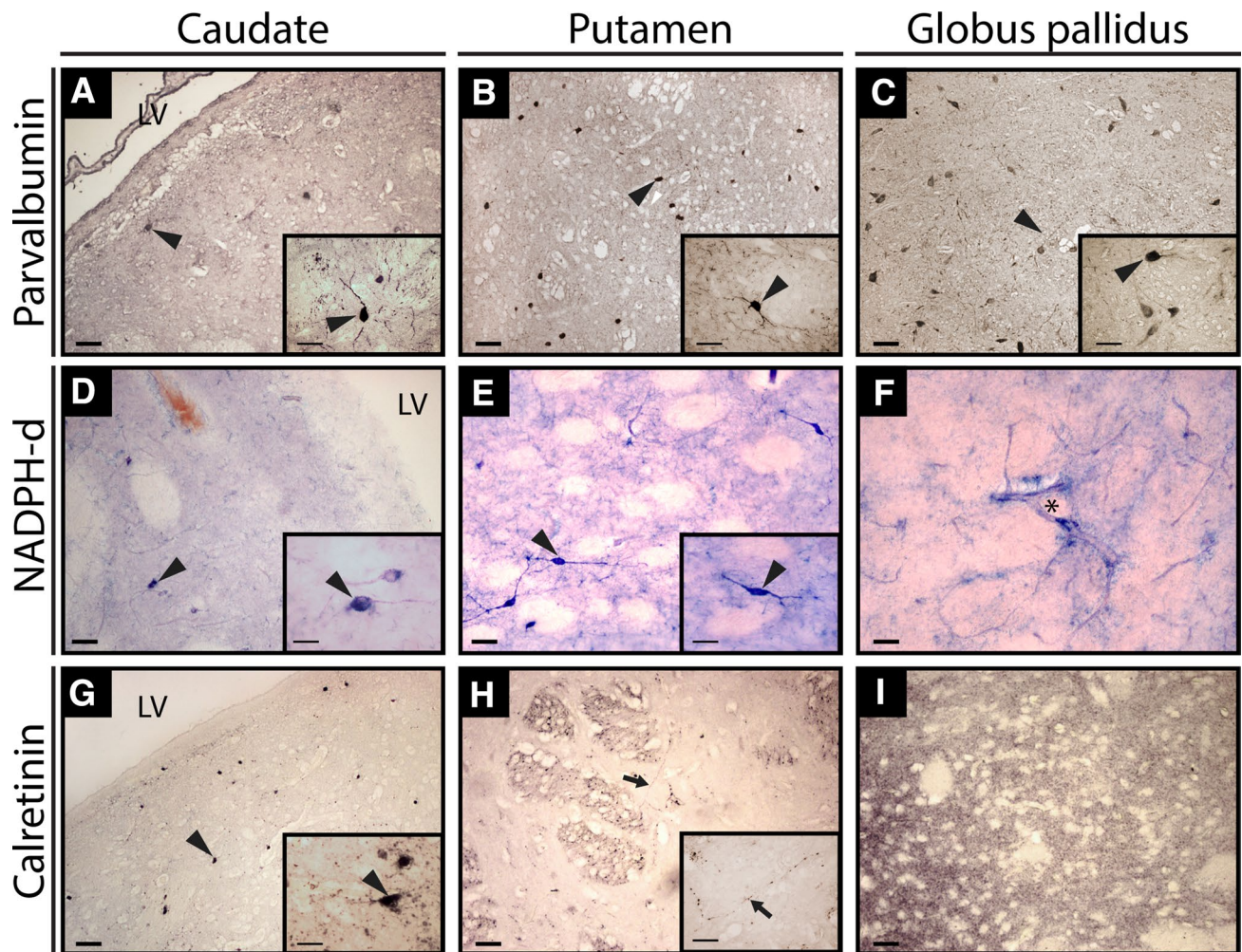


Fig. 4 Distribution of parvalbumin, NADPH-d and calretinin expression in the mid-striatum and globus pallidus of female vizcacha, *Lagostomus maximus*. Parvalbumin-immunoreactivity is observed in cells of the caudate nucleus (a), the putamen (b) and the globus pallidus (c). NADPH-d staining is observed in cells and matrix of the caudate nucleus (d) and the putamen (e); in the globus pallidus, NADPH-d staining was only detected in microvessels (f). Calretinin-immunoreactivity is differentially distributed in the striatum areas. In

the caudate nucleus, calretinin-immunoreactivity was detected in cells and neurofibers (g) and in the putamen, calretinin-immunoreactivity was detected in neurofibers of patches (h). In the globus pallidus, calretinin-immunoreactivity was detected in neuropil (i). Details of each immunoreactivity are shown in insets. Somatic immunoreactivity (arrowhead), neurofibrillar immunoreactivity (arrow) and NADPH-reactive microvessel (asterisk) are indicated. LV: lateral ventricle. Scale bars: 50 µm; insets scale bars: 10 µm

Table 3 Size and density of immunoreactive cells in the mid-striatum of the vizcacha, *L. maximus*

| Marker | Caudate | | | Putamen | | | Globus pallidus | | |
|---------|----------------|--------------|----------|----------------|--------------|----------|-----------------|--------------|---------|
| | SRA | MDRC | NRC | SRA | MDRC | NRC | SRA | MDRC | NRC |
| PV | 43.80 ± 10.83 | 7.37 ± 1.18 | 23 ± 6 | 48.2 ± 15.23 | 7.67 ± 1.46 | 50 ± 13 | 15.12 ± 4.94 | 4.35 ± 0.65 | 50 ± 15 |
| CR | 24.95 ± 5.38 | 6.89 ± 0.79 | 43 ± 14 | ND** | ND | ND | ND | ND | ND |
| CB | 56.71 ± 13.76 | 8.29 ± 0.74 | 440 ± 91 | 72.33 ± 13.57 | 9.42 ± 1.04 | 164 ± 31 | ND | ND | ND |
| GAD 65* | 114.95 ± 18.41 | 11.55 ± 0.75 | 11 ± 3 | 133.72 ± 61.35 | 12.46 ± 3.01 | 21 ± 5 | 113.67 ± 37.15 | 11.95 ± 2.11 | 59 ± 15 |
| GABA A | ND | ND | ND | ND | ND | ND | 96.5 ± 33.11 | 11.02 ± 2.33 | 26 ± 6 |

*Only strong stained GAD65-immunoreactive cells were counted

**ND not detected

The same six animals were analyzed for each marker. Values of average ± standard deviation are informed

CB Calbindin, CR Calretinin, GABA A ácido γ-aminobutírico receptor A, GAD 65 Glutamic acid decarboxylase 65, MDRC Medial Diameter of Reactive Cells (µm), NRC Number of Reactive Cells/10 mm², Parvalbumin, SRA somatic reactive area (µm²)

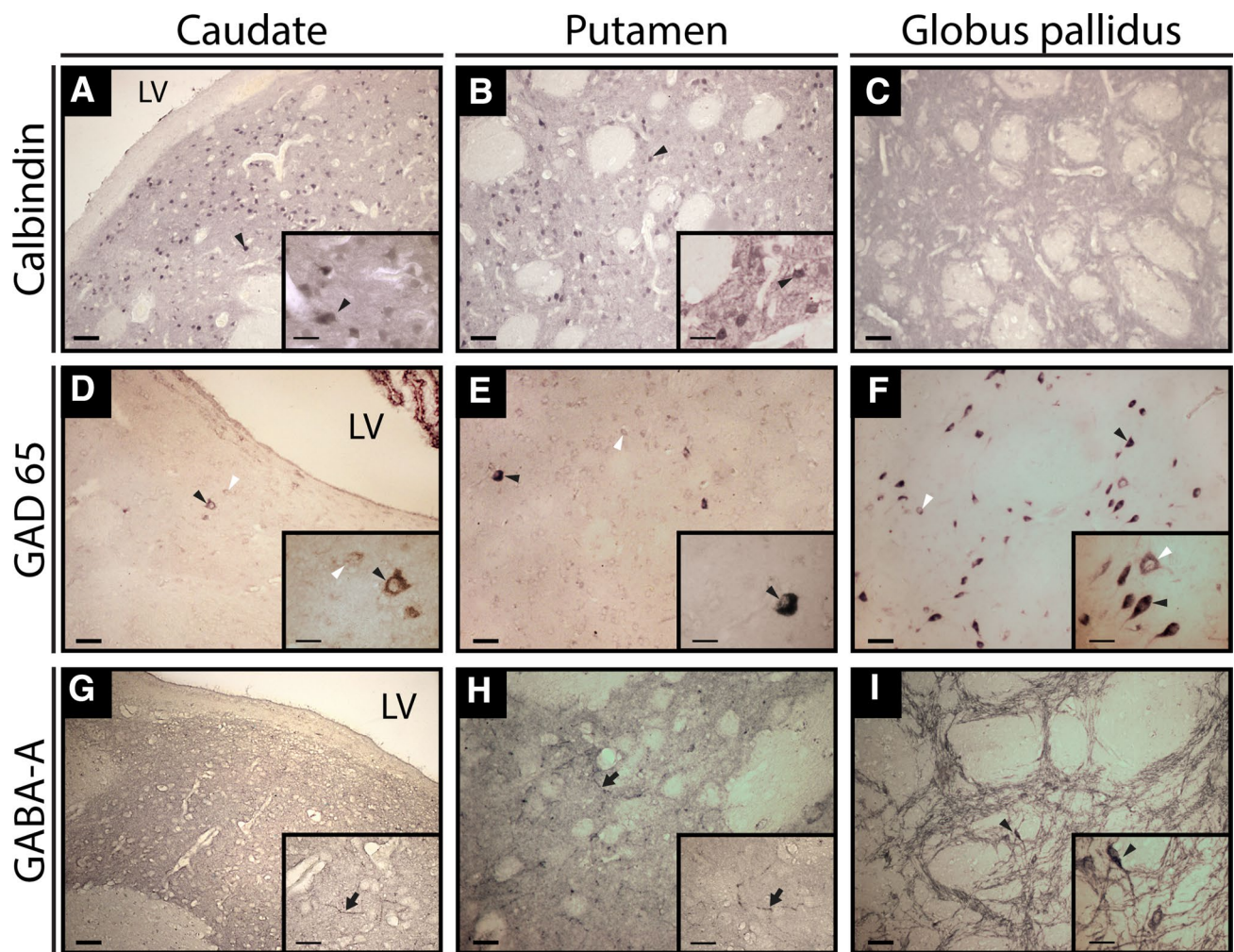


Fig. 5 Distribution of calbindin, GAD-65 and GABA-A expression in the mid-striatum and globus pallidus of female vizcacha, *Lagesotomus maximus*. Calbindin-immunoreactivity is observed in the somas of the matrix of the caudate nucleus (a) and the putamen (b); the globus pallidus showed only neuropil labeling (c). GAD-65-immunoreactivity is observed in cells located in the matrix of the striatum (d–e); and in cells of the globus pallidus (f). Two subpopulations of GAD65-immunoreactive cells were detected: mild immunoreactive

cells (white arrowheads) and strong immunoreactive cells (black arrowheads). GABA-A immunoreactivity is observed in neuropil and neurofibers of the matrix in the caudate nucleus (g) and the putamen (h). In addition, GABA-A immunoreactive neurofibers and bipolar cells were detected in the globus pallidus (i). Detail of each immunoreactivity is shown in insets. Somatic (arrowhead) and neurofibrillar immunoreactivity (arrow) is indicated. Scale bars: 50 μ m; insets scale bars: 10 μ m

pallidus and the substantia nigra, and aspiny interneurons expressing parvalbumin, NADPH-d, or calretinin, and controlling the action of projection neurons (Kawaguchi et al. 1995). This complex network of GABAergic cell bodies and processes detected in the striatum of the vizcacha had been previously found in other mammals (Kawaguchi et al. 1995; Rice et al. 2011). In addition, the immunoreactivity of the three calcium binding proteins parvalbumin, calretinin and calbindin, revealed a similar organization to the classical striosome–matrix cytoarchitecture in the striatum of vizcacha. The three neurochemical markers revealed ovoid cells, most of them devoid of visible immunoreactive dendrites, and a homogeneous matrix distribution without differences

of staining intensity among caudate and putamen as previously described for tree shrews (Rice et al. 2011). The differences in the distribution among calretinin-, calbindin-, and parvalbumin-immunoreactive cells may indicate different GABAergic pathways. Strikingly, GAD65-immunoreactive cells were much less abundant and bigger than calretinin-, calbindin-, and parvalbumin-immunoreactive cells, and the size is in range with the previously reported for other rodents, but is smaller than that described for the tree shrew and primates (Mensah and Deadwyler 1974; Yelniket al. 1991; Rice et al. 2011). However, the different size between GAD65-immunoreactive cells and calretinin-, calbindin-, and parvalbumin-immunoreactive cells may be related to

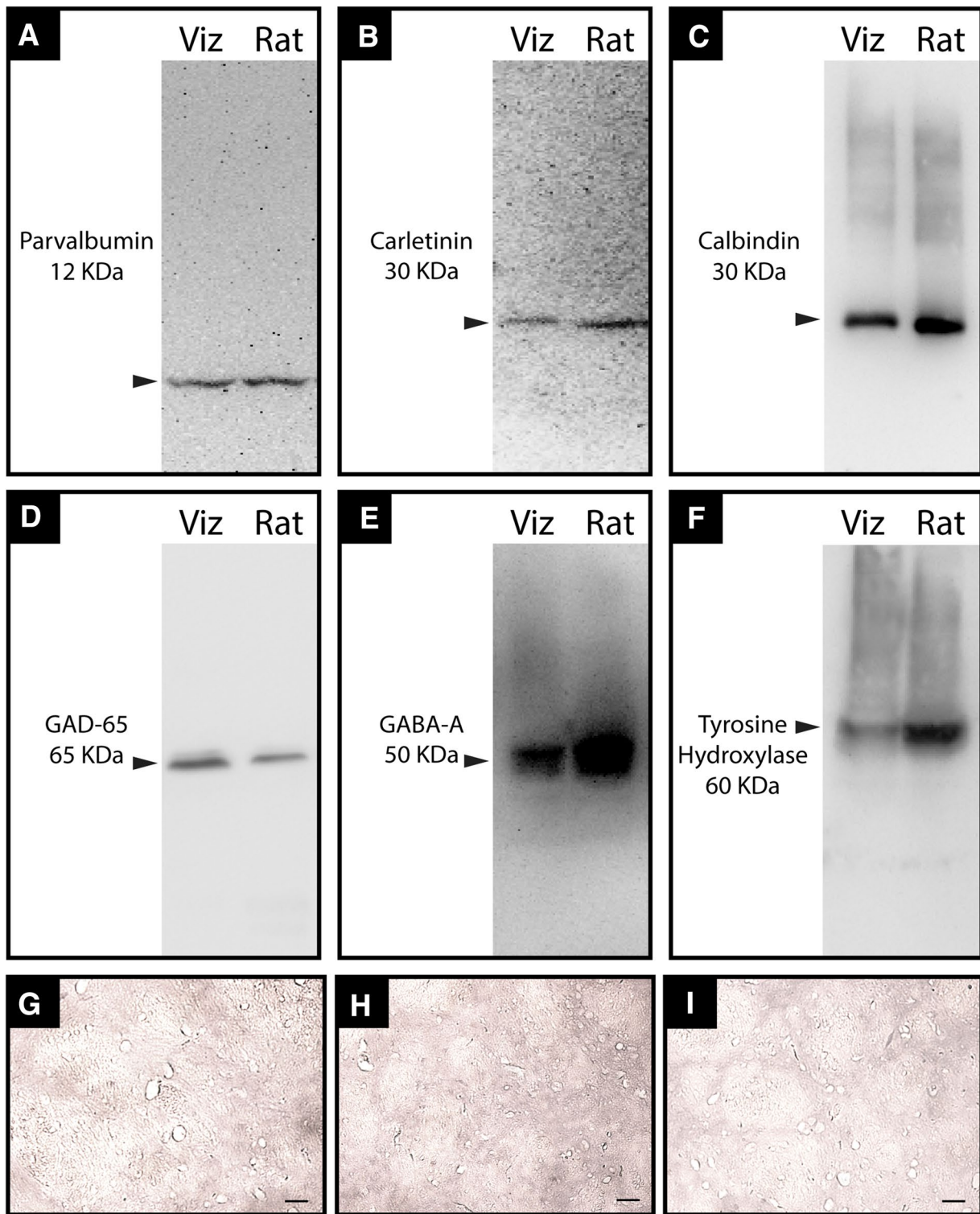


Fig. 6 Specific expression of parvalbumin, calretinin, calbindin, GAD-65, GABA-A, and tyrosine hydroxylase in the striatum of vizcacha, *Lagostomus maximus*. Representative images of protein expression of parvalbumin (a), calretinin (b), calbindin (c), GAD-65 (d), GABA-A (e), and tyrosine hydroxylase (f) determined by Western-blot in the striatum of non-pregnant vizcacha and non-pregnant rat (Sprague–Dawley). A pool of striatum proteins of one male rat

and one female rat (Rat), and a pool of striatum proteins of one male vizcacha and one female vizcacha (Viz) were used. Representative images of negative controls (primary antibodies omitted) of immunohistochemistry are shown in g (incubated with biotinylated anti-rabbit IgG), h (incubated with biotinylated anti-mouse IgG), and i (incubated with biotinylated anti-goat IgG)

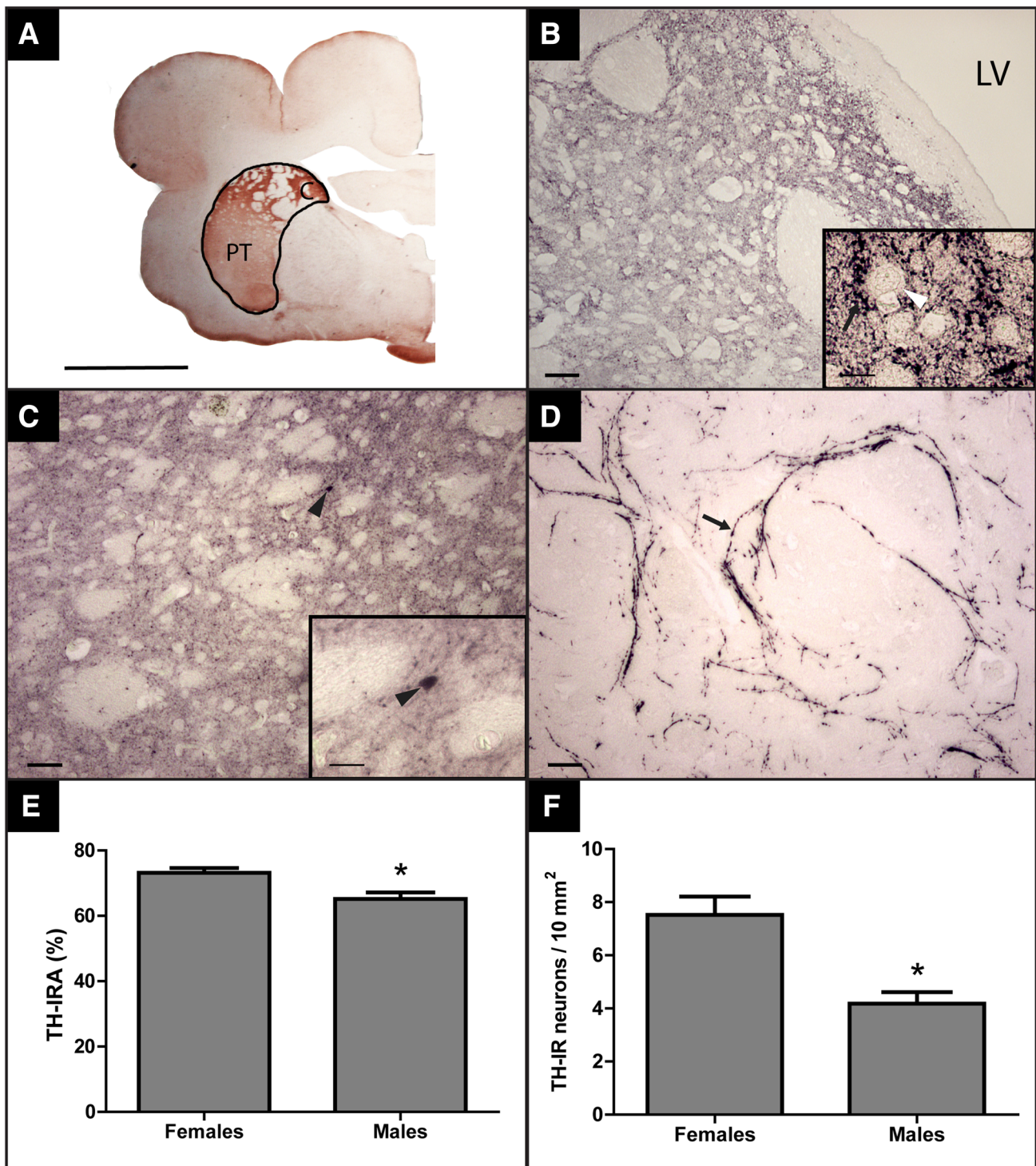


Fig. 7 Distribution of tyrosine hydroxylase (TH) expression and TH sexual dimorphism in the mid-striatum of vizcacha, *Lagostomus maximus*. TH-immunoreactivity is observed in the matrix of the caudate nucleus and the putamen (a–c). Caudate and putamen TH-immunoreactivity is enclosed by a black line (a). TH-immunoreactive terminals (arrow) surrounding a non-immunoreactive cell (white arrowhead) are observed in the inset (b). Small TH-immunoreactive cells are observed in the putamen (c). TH-immunoreactive neurofibers (arrow) are observed in the globus pallidus (d). Significantly larger mid-

striatum (caudate nucleus plus putamen) TH-immunoreactive area and significantly higher abundance of TH-immunoreactive cells was determined in females compared to males (e, f). Bars indicate average value \pm mean standard deviation. *T*-test was used to determine statistically significant differences between groups. Asterisks (*) indicate significant differences with $p < 0.05$. C: caudate nucleus. PT: putamen. Scale bars = (A): 5 mm (B): 100 μ m (C–D): 50 μ m, inset (B): 5 μ m, inset (C): 20 μ m

GAD67 activity which is, as well as GAD65, implicated in GABA synthesis. It should be considered that we did not study the expression of the enzyme GAD67. On the other hand, the presence of GABA-A immunoreactive cells exclusively located in the globus pallidus, confirms the inhibitory GABAergic modulation over this area (Parent and Hazrati 1995). In addition, neurons expressing the calcium binding proteins here analyzed (parvalbumin, calretinin and calbindin) were much more abundant and with a smaller size than the NADPH-d reactive neurons which showed similar size than GAD65-immunoreactive neurons. A similar distribution of NADPH-d staining at cells and neuropil of the caudate nucleus and the putamen was previously described in rat, cat and primates (Vincent and Johansson 1983; Sandell et al. 1986; Wu and Parent 2000).

Sexual dimorphism of TH expression

The expression of tyrosine hydroxylase (TH), the enzyme involved in the conversion of tyrosine in L-3,4 dihydroxyphenil alanina (L-DOPA), an intermediate of dopamine synthesis, has been reported in the striatum of mice and primates including humans (Dubach et al. 1987; Meredith et al. 1999; Cossette et al. 2005; Pickel et al. 1975; Xenias et al. 2015). Here we detected some scarce TH-immunoreactive cells in the putamen of male and female vizcachas. It has been described that gonadal hormones modulate TH and dopaminergic activity in the striatum. Accordingly, female rats and mice exhibit higher dopamine release than males (Walker et al. 1999; Arvidsson et al. 2014). Estradiol enhances striatal dopamine release in female rats without effects in males (McDermott et al. 1994; Becker 1999; Leranthe et al. 2000; Orendain-Jaime et al. 2016), whereas castrated male rats show higher striatum dopamine concentration than ovariectomized female rats (Xiao and Becker 1994). Here we showed sexual dimorphic expression of TH with a major expression area in the mid-striatum of females. Considering the modulatory effect of estrogens on dopamine induced sensorimotor function and behavior (Becker et al. 1987), and that we have recently shown the presence of aromatase in the brain of vizcacha (Charif et al. 2017), the sexual differences observed in this work may be related to the levels of estradiol and/or neuroestradiol available in the brain of vizcachas. Finally, the sex differences determined in the mid-striatum of vizcacha may have benefited the female survival. Female vizcachas take risks staying for long times outside the vizcachera searching for food and supervision of juvenile; unlike males spend most of the time inside the vizcachera or in its entrance fulfilling the role of observing and alerting through vocalization at the presence of predators (Branch 1993b; Jackson et al. 1996). Considering that the striatum is involved in the initiation and regulation of voluntary movements and motor learning, where dopamine

is associated with motor control, responses as reaction time for movements, decision making processes, motor learning, etc., could be related to the differences in tyrosine hydroxylase that would play a key role in influencing and favoring the specific female behavior in response to predators.

Evolutionary considerations

The striatum of vizcachas exhibits a clear regionalization resulting from the presence of an internal capsule that separates the striatum into the two well-defined structures: caudate nucleus and putamen. This strikingly differs from the undivided caudate–putamen structure seen in murids like mouse or rat and even in closer evolutionary related caviomorpha such as the guinea pig (*Cavia porcellus*) (Tindal 1965; Paxinos and Watson 2013). This regionalization of the striatum in *L. maximus*, reminds the anatomical organization found in other orders like Primates and Scandentia (Graybiel and Ragsdale 1978; Carpenter 1994; Snell 2007; Rice et al. 2011). It is worth to note that Primates, Scandentia, Rodentia and Lagomorpha originate from the same evolutionary clade. The presence of an internal capsule in the basal histricognathe *L. maximus*, makes a striking difference with laboratory conventional rodents such as mice and rats belonging to the myomorpha terminal clade in rodent phylogeny (Churakov et al. 2010; Voloch et al. 2013). In this way, the greater level of regionalization provided by the presence of the internal capsule may be correlated to a segregation of the motor and cognitive skills allowing the division of the striatal functions that would provide an adaptive advantage to the vizcacha (Daw et al. 2005; Dayan et al. 2006; Kreitzer and Malenka 2008; Liljeholm and O’Doherty 2012).

As it was suggested for the presence of brain convolutions that are lost in more recently evolved rodents, i.e. Myomorpha (Kelava et al. 2013), it seems reasonable to hypothesize a similar situation for the compartmentalization of the striatum. This feature would be an example of an evolutionary/phylogenetic constraint that emerged early and was retained in almost all groups except the murine rodents which likely underwent further modification to develop their unique striatal morphology. The greater degree of regionalization could be interpreted as an evolutive retention that enables the vizcacha’s lifestyle, since it allows an increase of motor skills for the construction of their caves and the manipulation of their food. Rodents with subterranean habits show morphological, physiological and ethological modifications as an adaptative response to the hypogeous environment that might still have impacted in their striatal biology as an adaptative advantage favouring escape from predators (Nevo 1979; Contreras 1981; Bee de Speroni and Pellegrini de Gastaldo 1988).

Acknowledgements We are especially grateful to the Ministerio de Asuntos Agrarios, Dirección de Flora y Fauna, Buenos Aires Province Government for enabling animal capture, to the personnel of ECAS for their invaluable help in trapping and handling the animals, to MV. Sergio Ferraris and MV. Fernando Lange and their veterinarian staff for their essential help on vizcachas handling and anesthetizing, to Ms. Sol Clausi Schettini for her excellent technical assistance in tissue processing, and Mr. Santiago Ciculli for his microscopy technical assistance. This work was funded by the National Scientific and Technical Research Council (CONICET): PIP No. 110/14, National Scientific and Technical Ministry (MINCYT): PICT-1281/2014, and by Fundación Científica Felipe Fiorellino, Universidad Maimónides, Argentina.

Compliance with ethical standards

Conflict of interest The authors declare that there is no conflict of interest.

References

- Arvidsson E, Viereckel T, Mikulovic S, Wallen-Mackenzie A (2014) Age- and sex-dependence of dopamine release and capacity for recovery identified in the dorsal striatum of C57/Bl6J mice. *PLoS ONE* 9(6):e99592
- Bae EJ, Chen BH, Shin BN, Cho JH, Kim IH, Park JH, Lee JC, Tae HJ, Choi SY, Kim JD, Lee YL, Won MH, Ahn JH (2015) Comparison of immunoreactivities of calbindin-D28k, calretinin and parvalbumin in the striatum between young, adult and aged mice, rats and gerbils. *Neurochem Res* 40(4):864–872
- Becker JB (1999) Gender differences in dopaminergic function in striatum and nucleus accumbens. *Pharmacol Biochem Behav* 64:803–812
- Becker JB, Snyder PJ, Miller MM, Westgate SA, Jenuwine MJ (1987) The influence of estrous cycle and intrastratial estradiol on sensorimotor performance in the female rat. *Pharmacol Biochem Behav* 27:53–59
- Bee de Speroni N, Pellegrini de Gastaldo A (1988) Encefalización y composición cerebral en tres roedores sudamericanos (*Dolichotis patagonum*, *Lagostomus maximus* y *Calomys musculus*). *Physis* 46(111):31–39
- Bradford MM (1976) Rapid and sensitive method for the quantitation of microgram quantities of protein utilizing the principle of protein-dye binding. *Anal Biochem* 72:248–254
- Branch LC (1993a) Social organization and mating system of the plains viscacha (*Lagostomus maximus*). *J Zool (London)* 229:473–491
- Branch LC (1993b) Seasonal patterns of activity and body mass in plains viscacha, *Lagostomus maximus* (family Chinchillidae). *Can J Zool* 71:1041–1045
- Branch LC (1995) Observations of predation by pumas and Geoffroy's cats on the plains vizcacha in semiarid scrub of central Argentina. *Mammalia* 59:152–156
- Carpenter MB (1994) *Neuroanatomía: fundamentos* 4th edition. Médica Panamericana. 448 pag. ISBN: 9788479031732.
- Charif SE, Insera PIF, Schmidt AR, Di Giorgio NP, Cortasa SA, Gonzalez CR, Lux-Lantos V, Halperin J, Vitullo AD, Dorfman VB (2017) Local production of neuroestradiol affects gonadotropin-releasing hormone (GnRH) secretion at mid-gestation in *Lagostomus maximus* (Rodentia, Caviomorpha). *Physiol Rep* 5(19):e13439
- Charif SE, Insera PIF, Di Giorgio NP, Schmidt AR, Lux-Lantos V, Vitullo AD, Dorfman VB (2016) Sequence analysis, tissue distribution and molecular physiology of the GnRH preprogonadotrophin in the South American plains vizcacha (*Lagostomus maximus*). *Gen Comp Endocrinol* 232:174–184
- Churakov G, Sadasivuni MK, Rosenbloom KR, Huchon D, Brosius J, Schmitz J (2010) Rodent evolution: back to the root. *Mol Biol Evol* 27:1315–1326
- Contreras JR (1981) El tunduque: Un modelo de ajuste adaptativo. *Serie Científica* 22–25.
- Cossette M, Lecomte F, Parent A (2005) Morphology and distribution of dopaminergic neurons intrinsic to the human striatum. *J Chem Neuroanat* 29:1–11
- Daubner SC, Le T, Wang S (2011) Tyrosine hydroxylase and regulation of dopamine synthesis. *Arch Biochem Biophys* 508(1):1–12
- Daw ND, Niv Y, Dayan P (2005) Uncertainty-based competition between prefrontal and dorsolateral striatal systems for behavioral control. *Nat Neurosci* 8:1704–1711
- Dayan P, Niv Y, Seymour B, Daw ND (2006) The misbehavior of value and the discipline of the will. *Neural Netw* 19:1153–1160
- De las Heras S, Hontanilla B, Mengual E, Giménez-Amaya JM (1994) Immunohistochemical distribution of calbindin D-28k and parvalbumin in the head of the caudate nucleus and substantia nigra of the cat. *J Morphol* 221(3):291–307
- DeLong M, Alexander GE, Georgopoulos AP, Crutcher MD, Mitchell SJ, Richardson RT (1984) Role of basal ganglia in limb movements. *Hum Neurobiol* 2:235–244
- DeLong MR, Georgopoulos AP (1981) Motor functions of the basal ganglia. *Handb Physiol* 3:1017–1061
- Dorfman VB, Fraunhofer N, Insera PIF, Loidl CF, Vitullo AD (2011) Histological characterization of gonadotropin-releasing hormone (GnRH) in the hypothalamus of the South American plains vizcacha (*Lagostomus maximus*). *J Mol Histol* 42:311–321
- Dorfman VB, Saucedo L, Di Giorgio NP, Insera PIF, Fraunhofer N, Leopardo NP, Halperin J, Lux-Lantos V, Vitullo AD (2013) Variation in progesterone receptors and GnRH expression in the hypothalamus of the pregnant South American plains vizcacha, *Lagostomus maximus* (Mammalia, Rodentia). *Biol Reprod* 89(5):115–125
- Dubach M, Schmidt R, Kunkel D, Bowden DM, Martin R, German DC (1987) Primate neostriatal neurons containing tyrosine hydroxylase: immunohistochemical evidence. *Neurosci Lett* 75:205–210
- Fujiyama F, Unzai T, Nakamura K, Nomura S, Kaneko T (2006) Difference in organization of corticostriatal and thalamostriatal synapses between patch and matrix compartments of rat neostriatum. *Eur J Neurosci* 24:2813–2824
- Gerfen CR (1984) The neostriatal mosaic: compartmentalization of corticostriatal input and striatonigral output systems. *Nature* 311:461–464. <https://doi.org/10.1038/311461a0>
- Gerfen CR, Wilson CJ (1996) The Basal Ganglia. In: Hokfelt T, Swanson LW (eds) *Handbook of Chemical Neuroanatomy*. Elsevier, Amsterdam, pp 365–462
- Gillies A, Willshaw D, Li Z (2002) Subthalamic-pallidal interactions are critical in determining normal and abnormal functioning of the basal ganglia. *Proc Biol Sci* 269(1491):545–551
- Gonzalez CR, Muscársel Isla ML, Fraunhofer NA, Leopardo NP, Vitullo AD (2012a) Germ cell differentiation and proliferation in the developing testis of the South American plains viscacha, *Lagostomus maximus* (Mammalia, Rodentia). *Zygote* 20(3):219–227
- Gonzalez CR, Muscársel Isla ML, Leopardo NP, Willis MA, Dorfman VB, Vitullo AD (2012b) Expression of androgen receptor, estrogen receptors alpha and beta and aromatase in the fetal, perinatal, prepubertal and adult testes of the South American plains vizcacha, *Lagostomus maximus* (Mammalia, Rodentia). *J Reprod Dev* 58(6):629–635
- Gonzalez CR, Muscársel Isla ML, Vitullo AD (2018) The balance between apoptosis and autophagy regulates testis regression and recrudescence in the seasonal-breeding South American plains vizcacha, *Lagostomus maximus*. *PLoS ONE* 13(1):e0191126

- Graybiel AM (1983) Compartmental organization of the mammalian striatum. *Prog Brain Res* 58:247–256
- Graybiel AM (1990) Neurotransmitters and neuromodulators in the basal ganglia. *Trends Neurosci* 13:244–254. [https://doi.org/10.1016/0166-2236\(90\)90104-I](https://doi.org/10.1016/0166-2236(90)90104-I)
- Graybiel AM (2008) Habits, rituals, and the evaluative brain. *Annu Rev Neurosci* 31:359–387. <https://doi.org/10.1146/annurev.neuro.29.051605.112851>
- Graybiel AM, Ragsdale CW (1978) Histochemically distinct compartments in the striatum of human, monkey and cat demonstrated by acetylthiocholinesterase staining. *Proc Natl Acad Sci* 75(11):5723–5726
- Halperin J, Dorfman VB, Fraunhoffer N, Vitullo AD (2013) Estradiol, progesterone and prolactin modulate mammary gland morphogenesis in adult female plains vizcacha (*Lagostomus maximus*). *J Mol Histol* 44(3):299–310
- Herkenham M, Pert CB (1981) Mosaic distribution of opiate receptors, parafascicular projections and acetylcholinesterase in rat striatum. *Nature* 291:415–418. <https://doi.org/10.1038/291415a0>
- Holt DJ, Graybiel AM, Saper CB (1997) Neurochemical architecture of the human striatum. *J Comp Neurol* 384:1–25
- Insera PIF, Charif SE, Di Giorgio NP, Saucedo L, Schmidt AR, Fraunhoffer N, Halperin J, Gariboldi MC, Leopardo NP, Lux-Lantos V, Gonzalez CR, Vitullo AD, Dorfman VB (2017) ER α and GnRH co-localize in the hypothalamic neurons of the South American plains vizcacha, *Lagostomus maximus* (Rodentia, Caviomorpha). *J Mol Histol* 48(3):259–273
- Jackson JE (1986) Determinación de edad en la vizcacha (*Lagostomus maximus*) en base al peso del cristalino. *Vida Silvestre Neotropical* 1:41–44
- Jackson JE, Lyn C, Villarreal D (1996) *Lagostomus maximus* mammalian. *Species* 543:1–6
- Jensen F, Willis MA, Albamonte MS, Espinosa MB, Vitullo AD (2006) Naturally suppressed apoptosis prevents follicular atresia and oocyte reserve decline in the adult ovary of *Lagostomus maximus* (Rodentia, Caviomorpha). *Reproduction* 132:301–308
- Kawaguchi Y, Wilson CJ, Augood SJ, Emson PC (1995) Striatal interneurons: chemical, physiological and morphological characterization. *Trends Neurosci* 18(12):527–535
- Kelava I, Lewitus E, Huttner WB (2013) The secondary loss of gyrencephaly as an example of evolutionary phenotypical reversal. *Front Neuroanat* 7:16
- Kita H, Jaeger D (2016) Organization of the Globus Pallidus. *Handb Behav Neurosci* 24:259–276. <https://doi.org/10.1016/B978-0-12-802206-1.00013-1>
- Kubota Y, Inagaki S, Kito S (1986) Innervation of substance P neurons by catecholaminergic terminals in the neostriatum. *Brain Res* 375:163–167. [https://doi.org/10.1016/0006-8993\(86\)90969-8](https://doi.org/10.1016/0006-8993(86)90969-8)
- Kubota Y, Kawaguchi Y (1993) Spatial distributions of chemically identified intrinsic neurons in relations to patch and matrix compartments of rat neostriatum. *J Comp Neurol* 332:499–513. <https://doi.org/10.1002/cne.903320409>
- Klüver H, Barrera E (1953) A method for the combined staining of cells and fibers in the nervous system. *J Neuropathol Exp Neurol* 12:400–403
- Kreitzer AC, Malenka RC (2008) Striatal plasticity and basal ganglia circuit function. *Neuron* 60(4):543–554
- Lavoie B, Parent A (1990) Immunohistochemical study of the serotonergic innervation of the basal ganglia in the squirrel monkey. *J Comp Neurol* 1:1. <https://doi.org/10.1111/eip.12846>
- Leranth C, Roth RH, Elsworth JD, Naftolin F, Horvath TL, Redmond DE Jr (2000) Estrogen is essential for maintaining nigrostriatal dopamine neurons in primates: implications for Parkinson's Disease and memory. *J Neurosci* 20(23):8604–8609
- Liljeholm M, O'Doherty JP (2012) Contributions of the striatum to learning, motivation and performance: an associative account. *Trends Cogn Sci* 16(9):467–475
- Llanos AC, Crespo JA (1952) Ecología de la vizcacha (*Lagostomus maximus maximus* Blainv.) en el nordeste de la Provincia de Entre Ríos. *Revista de Investigaciones Agrícolas* 6:289–378
- Luparello TJ, Stein M, Park CD (1964) A stereotaxic atlas of the hypothalamus of the guinea pig. *J Comp Neurol* 122:201–217
- McDermott JL, Liu B, Dluzen DE (1994) Sex differences and effects of estrogen on dopamine and DOPAC release from the striatum of male and female CD-1 mice. *Exp Neurol* 125:306–311
- Mensah P, Deadwyler S (1974) The caudate nucleus of the rat: cell types and the demonstration of a commissural system. *J Anat* 117:281–293
- Meredith GE, Farrell T, Kellaghan P, Tan Y, Zahm DS, Totterdell S (1999) Immunocytochemical characterization of catecholaminergic neurons in the rat striatum following dopamine-depleting lesions. *Eur J Neurosci* 10:3585–3596
- Micheli FE and Luquin-Piudo ME (2012) Functional organization of basal ganglia. *Abnormal movements*. Ed: Medica Panamericana, Chapter 2.
- Middleton FA, Strick PL (1994) Anatomical evidence for cerebellar and basal ganglia involvement in higher cognitive function. *Science* 226:452–461
- Nevo E (1979) Adaptive convergence and divergence of subterranean mammals. *Annu Rev Ecol Evol Syst* 10:269–308
- National Research Council USA (2011) Guide for the care and use of laboratory animals, 8th edn. The National Academies Press, Washington
- Orendain-Jaime EN, Ortega-Ibarra JM, López-Pérez SJ (2016) Evidence of sexual dimorphism in D1 and D2 dopaminergic receptors expression in frontal cortex and striatum of young rats. *Neurochem Int* 100:62–66
- Parent A, Hazrati LN (1995) Functional anatomy of the basal ganglia. I. The cortico-basal ganglia-thalamo-cortical loop. *Brain Res Rev* 20:91–127
- Paxinos G, Watson C (2013) The rat brain in stereotaxic coordinates. AP press, Amsterdam
- Paxinos G, Franklin KBJ (2004) The mouse brain in stereotaxic coordinates. Elsevier Academic Press, Amsterdam
- Rey-Funes M, Dorfman VB, Ibarra ME, Peña E, Contartese DE, Goldstein J, Acosta JM, Larráyoiz I, Martínez-Murillo R, Martínez A, Loidl CF (2013) Hypothermia prevents gliosis and angiogenesis development in an experimental model of ischemic proliferative retinopathy. *Invest Ophthalmol Vis Sci* 54(4):2836–2846
- Rey-Funes M, Larráyoiz I, Fernández J, Contartese D, Rolón F, Insera PIF, Martínez-Murillo R, López-Costa J, Dorfman VB, Martínez A, Loidl CF (2016) Methylene blue prevents retinal damage in an experimental model of ischemic proliferative retinopathy. *Am J Physiol Regul Integr Comp Physiol* 310(11):R1011–1019
- Rice MW, Roberts RC, Melendez-Ferro M, Perez-Costas E (2011) Neurochemical characterization of the tree shrew dorsal striatum. *Front Neuroanat* 5:1–16
- Sandell JH, Graybiel AM, Chesselet MF (1986) A new enzyme marker for striatal compartmentalization: NADPH diaphorase activity in the caudate nucleus and putamen of the cat. *J Comp Neurol* 243:326–334
- Smith Y, Bevan MD, Shink E, Bolam JP (1998) Microcircuitry of the direct and indirect pathways of the basal ganglia. *Neuroscience* 86(2):353–387
- Snell RS (2007) *Neuroanatomía clínica* 6 ed. Medica Panamericana, p 594
- Tindal JS (1965) The forebrain of the guinea pig in stereotaxic coordinates. *J Comp Neurol* 124:259–256
- Vincent SR, Johansson O (1983) Striatal neurons containing both somatostatin and avian pancreatic polypeptide APPI-like

- immunoreactivities and NADPH diaphorase activity: a light and electron microscopic study. *J Comp Neurol* 217:264–270
- Voloch CM, Vilela JF, Loss-Oliveira L, Schrago CG (2013) Phylogeny and chronology of the major lineages of New World hystricognath rodents: insights on the biogeography of the Eocene/Oligocene arrival of mammals in South America. *BMC Res Notes* 6:160
- Walker QD, Rooney MB, Wightman RM, Kuhn CM (1999) Dopamine release and uptake are greater in female than male rat striatum as measured by fast cyclic voltammetry. *Neuroscience* 95(4):1061–1070
- Wu Y, Parent A (2000) Striatal interneurons expressing calretinin, parvalbumin or NADPH-diaphorase: a comparative study in the rat, monkey and human. *Brain Res* 863(1–2):182–191
- Xenias HS, Ibáñez-Sandoval O, Koós T, Tepper JM (2015) Are striatal tyrosine hydroxylase interneurons dopaminergic? *J Neurosci* 35(16):6584–6599
- Xiao L, Becker JB (1994) Quantitative microdialysis determination of extracellular striatal dopamine concentrations in male and female rats: effects of estrous cycle and gonadectomy. *Neurosci Lett* 180:155–158
- Yelnik J, Francois C, Percheron G, Tande D (1991) Morphological taxonomy of the neurons of the primate striatum. *J Comp Neurol* 313:273–294

Publisher's Note Springer Nature remains neutral with regard to jurisdictional claims in published maps and institutional affiliations.